Acknowledgment. We thank the Department of Energy, Office of Basic Energy Sciences, for support of this research and the donors of the Petroleum Research Fund, administered by the American Chemical Society, for an undergraduate summer research fellowship to C.A.M. Also acknowledged are the National Science Foundation for contributing funds toward the purchase of the diffractometer at the University of Delaware, G. Steinmetz and R. Hale (Tennessee Eastman Co.) for obtaining mass spectra, and A. Freyer (Penn State) for assistance with the ^1H NMR saturation-transfer experiments. The DANTE ^{13}C saturation-transfer experiment was performed at the National Science Foundation Regional Facility in NMR at the University of South Carolina (Grant No. CHE 82-07445). We gratefully acknowledge the assistance of Drs. Alan Benesi and Helga Cohen in obtaining these results.

Registry No. 1, 77208-32-3; 2, 104324-86-9; 5, 104324-87-0; $Pt(PPh_3)_2(CH_2{=}CH_2)$, 12120-15-9; Os, 7440-04-2; Pt, 7440-06-4.

Supplementary Material Available: Tables of anisotropic temperature factors, bond lengths and angles, and hydrogen atom coordinates and a plot of kinetic data from the ^1H NMR magnetization transfer experiment for 2 (5 pages); a list of structure factors (19 pages). Ordering information is given on any current masthead page.

Reactions of $(\mu\text{-H})_2Rh_2[P(O\text{-}i\text{-}Pr)_3]_4$ with Hydrogen. A Novel Isocyanide Hydrogenation Reaction

Stephen T. McKenna,*† Richard A. Andersen, and Earl L. Muetterties‡

Department of Chemistry, University of California, Berkeley, California 94720

Received November 5, 1985

The reaction of the compounds $(\mu\text{-H})_2(RNC)Rh_2[P(O\text{-}i\text{-}Pr)_3]_4$ (R = 4-ClC_6H_4, $PhCH_2$) with H_2 yields $(\mu\text{-H})(\mu\text{-RNMe})Rh_2[P(O\text{-}i\text{-}Pr)_3]_4$, formally the result of transfer of three hydrogens to the isocyanide carbon and reduction of the triple bond to a single bond. The X-ray crystal structure of $(\mu\text{-H})(\mu\text{-4-}ClC_6H_4NMe)Rh_2[P(O\text{-}i\text{-}Pr)_3]_4$ (monoclinic, $P2_1/n$, a = 13.960 (2) Å, b = 19.430 (2) Å, c = 21.825 (2) Å, β = 91.36 (1)°, Z = 4; R = 0.042, R_w = 0.056 for 5098 data with $I > 3\sigma$) shows two RhP_2 units bridged by the arylmethylamido group and the hydride (not located) with a geometry slightly twisted out of planarity. The intermediate in the reaction, the formimidoyl species $H(\mu\text{-H})_2(RN{=}CH)Rh_2[P(O\text{-}i\text{-}Pr)_3]_4$, can be detected by multinuclear NMR. Upon further reaction with H_2, low conversions to the secondary amines RNHMe plus $H(\mu\text{-H})_3Rh_2[P(O\text{-}i\text{-}Pr)_3]_4$ are observed. Reaction of $(\mu\text{-H})(\mu\text{-RNMe})Rh_2[P(O\text{-}i\text{-}Pr)_3]_4$ with additional RNC results in a mixture of $(\mu\text{-H})(\mu\text{-RNMe})Rh[P(O\text{-}i\text{-}Pr)_3]_3(RNC)$, the result of substitution of a phosphite by RNC, and mononuclear products. For the reaction of $(\mu\text{-H})_2(RNC)Rh_2[P(O\text{-}i\text{-}Pr)_3]_4$ (R = *n*-Bu, *t*-Bu, and 2,6-$Me_2C_6H_3$) with H_2, substitution and fragmentation processes compete with the hydrogenation reaction and little or no $(\mu\text{-H})(\mu\text{-RNMe})Rh_2[P(O\text{-}i\text{-}Pr)_3]_4$ is produced. Under D_2, the complexes $(\mu\text{-H})(\mu\text{-RNMe})Rh_2[P(O\text{-}i\text{-}Pr)_3]_4$ display H/D exchange via an intramolecular oxidative addition process which results in selective D incorporation into the phosphite methyl positions, as well as the ortho and benzylic positions of the amido ligand in the compound with R = $PhCH_2$.

Introduction

The reduction of C≡O and C≡N triple bonds is a process of extreme practical importance. However, unlike C≡C triple bond hydrogenation, for which homogeneous catalytic processes are well-known,[1-3] useful soluble catalysts for reducing C≡O and C≡N triple bonds are rare. Complexes of the form $HRhP_2$ have been found to catalyze the hydrogenation of nitriles to primary amines under mild conditions;[4] hydridoruthenium phosphine complexes are reported to do the same under more forcing conditions.[5] The clusters $Ni_4(RNC)_7$ catalyze the hydrogenation of isocyanides to secondary amines.[6] Catalytic systems for the hydrogenation of CO to alcohols[7,8] or alkanes[9] have been reported, but conditions are typically severe and the natures of the active species are unclear. In none of these cases are mechanistic details known.

A stoichiometric hydrogenation of CO to bound methoxide has been observed by Bercaw and co-workers.[10] The reaction of $[(C_5Me_5)_2Zr(N_2)]_2(\mu\text{-}N_2)$ with CO followed by H_2 appears to proceed by attack of $(C_5Me_5)_2ZrH_2$ on the proposed intermediate formyl complex $(C_5Me_5)_2Zr(H)$-(CHO) to give $(C_5Me_5)_2Zr(H)(OMe)$. Under slightly different conditions, the unique binuclear enediolate complex

Scheme I

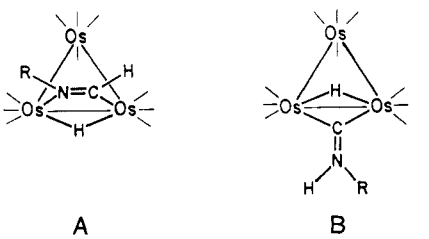

A B

† Address correspondence to this author at Amoco Research Center, P.O. Box 400, Naperville, IL 60566.

‡ Deceased January 12, 1984.

(1) (a) Collmann, J. P.; Hegedus, L. *Principles and Applications of Organotransition Metal Chemistry*; University Science Books: Mill Valley, CA, 1980. (b) Parshall, G. W. *Homogeneous Catalysis*; Wiley: New York, 1980.

(2) Muetterties, E. L.; Krause, M. J. *Angew. Chem., Int. Ed. Engl.* **1983**, *22*, 135.

(3) (a) Burch, R. R.; Muetterties, E. L.; Teller, R. G.; Williams, J. M. *J. Am. Chem. Soc.* **1982**, *104*, 4257. (b) Burch, R. R.; Shusterman, A. J.; Muetterties, E. L.; Teller, R. G.; Williams, J. M. *J. Am. Chem. Soc.* **1983**, *105*, 3546.

(4) Yoshida, T.; Okano, T.; Otsuka, S. *J. Chem. Soc., Chem. Comm.* **1979**, 870.

(5) Grey, R. A.; Pez, G. P.; Wallo, A. *J. Am. Chem. Soc.* **1981**, *103*, 7536.

0276-7333/86/2305-2233$01.50/0

$(C_5Me_5)_2Zr(H)[\mu\text{-}OC(H)=C(H)O](H)Zr(C_5Me_5)_2$ is formed instead. An analogue of this reaction was found in the reduction of isocyanides by $(C_5Me_5)_2ZrH_2$.[11] Isocyanides were found to insert into a Zr–H bond of the starting complex even at low temperatures, affording the formimidoyl complexes $(C_5Me_5)_2Zr(H)(HC=NR)$. In the case of R = 2,6-$Me_2C_6H_3$, a second insertion was observed to give the methyleneimine complex $(C_5Me_5)_2Zr(\eta^2\text{-}CH_2NR)$. Reaction with hydrogen then led to further reduction to $(C_5Me_5)_2Zr(H)(NRMe)$. Thus all three separate hydrogen transfers to the isocyanide carbon were observed and a clear picture of the reaction was obtained.

Individual steps of the nitrile and isonitrile reduction processes have been reported in other systems. The most commonly observed step is the first hydrogen transfer, giving formimidoyl (–HC=NR) or iminyl (=C=NHR) ligands from isocyanides and acimidoyl (–RC=NH) or alkylidenimido (–N=CHR) ligands from nitriles. A number of platinum[12–15] and ruthenium[16] hydrides react with isocyanides to give formimidoyl species. Among transition-metal clusters, hydrides of Fe_3,[17] Ru_3,[18] and Os_3[19] clusters react with isocyanides to yield formimidoyl and iminyl species. The system of Adams and Golembeski[19] is relatively well-characterized (Scheme I). Isocyanides react with $(\mu\text{-}H)_2Os_3(CO)_{10}$ initially by forming a simple adduct, $H(\mu\text{-}H)Os_3(CO)_{10}(RNC)$. Upon heating, one of two insertion pathways is followed. In nonpolar solvents, the isocyanide appears to insert directly into an Os–H bond, giving a formimidoyl ligand which binds to two Os atoms in σ,σ fashion through its C and N atoms (structure A). If the adduct is heated in polar solvents, a different course is followed. The adduct is deprotonated and the isocyanide moves to a bridging position between two Os atoms. It is then reprotonated at nitrogen rather than at osmium, yielding a $\mu\text{-}\eta^1$-iminyl ligand (structure B). Similar chemistry has been seen with nitriles by Kaesz[20] for Fe_3 clusters and by Vahrenkamp[21] for Ru_3 clusters. In both cases, initial insertion gave $\mu\text{-}\eta^1$-alkylidenimido ligands; in the Fe_3 case, a $\mu_3\text{-}\eta^2$-acimidoyl complex was formed as well. Hydrogenation of the alkylidenimido complexes led to further reduction to the C–N single bonded species $(\mu\text{-}H)_2(\mu_3\text{-}RCH_2N)M_3(CO)_9$.

Thus it appears that further reduction of an isocyanide requires the availability of an additional coordination site for the intermediate formimidoyl or alkylidenimido moiety.[22] This may be accomplished either in mononuclear complexes such as the $(C_5Me_5)_2Zr$ system, where the intermediate may be η^2-bound, or in polynuclear complexes, where $\mu\text{-}\eta^2$ and $\mu_3\text{-}\eta^2$ binding are also possible. The isocyanide adducts of $(\mu\text{-}H)_2Rh_2[P(O\text{-}i\text{-}Pr)_3]_4$,[23] $(\mu\text{-}H)_2(RNC)Rh_2[P(O\text{-}i\text{-}Pr)_3]_4$ (**1a**, R = 4-ClC_6H_4; **1b**, R = $PhCH_2$; **1c**, R = *n*-Bu; **1d**, R = *t*-Bu; **1e**, R = 2,6-$Me_2C_6H_3$),[24] appear to be logical candidates for such reductions due to their coordinative unsaturation. Accordingly the reactions of **1a–e** and related compounds with hydrogen were explored.

Scheme II

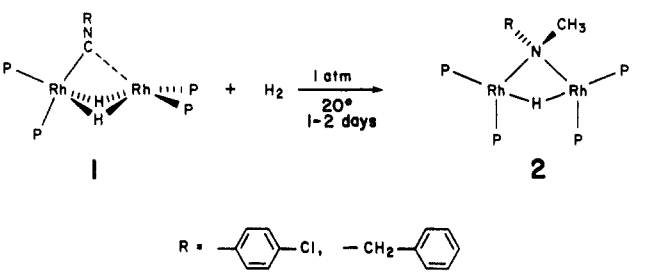

Table I. Crystal and Data Collection Parameters for 2a, $(\mu\text{-}H)(\mu\text{-}4\text{-}ClC_6H_4NCH_3)Rh_2[P(O\text{-}i\text{-}Pr)_3]_4$

Crystal Data	
formula: $C_{43}H_{92}ClNO_{12}P_4Rh_2$	fw: 1180.36
Crystal Parameters at 25 °C	
a = 13.960 (2) Å	space group: $P2_1/n$
b = 19.430 (2) Å	Z = 4
c = 21.825 (2) Å	d_{calcd} = 1.32 g/cm^3
β = 91.36 (1)°	μ_{calcd} = 7.49 cm^{-1}
$\alpha = \gamma$ = 90°	size: 0.42 × 0.27 × 0.11 mm
Data Measurement and Structure Solution	
diffractometer: Enraf-Nonius CAD-4	
radiation: Mo Kα (λ = 0.71073 Å)	
monochromator: graphite	
reflections measured: $+h,+k,\pm l$	
2θ range: 2–45°	
scan type: θ–2θ	
scan speed: variable from 0.7 to 6.7°/min	
scan width: $\Delta\theta$ = 0.60 + 0.35 tan θ°	
bkgd: additional 0.25($\Delta\theta$) at each end of scan	
no. of reflctns collected (including standards): 8571	
no. of unique reflctns: 7712	
no. with $I > 3\sigma(I)$: 5098	
no. of parameters: 568	
final residuals[25]: R = 0.042; R_w = 0.056; GOF = 1.67	

Results and Discussion

Formation and Properties of $(\mu\text{-}H)(\mu\text{-}RNMe)Rh_2[P(O\text{-}i\text{-}Pr)_3]_4$ (2a,b). The compounds $(\mu\text{-}H)_2(RNC)Rh_2[P(O\text{-}i\text{-}Pr)_3]_4$ (**1a**, R = 4-ClC_6H_4; **1b**, R = $PhCH_2$), whose structures[24] are shown in Scheme II, react with 1 atm of hydrogen in hydrocarbon solvents over the course of 1–2 days at 20 °C to give good yields of the yellow

(6) (a) Band, E.; Pretzer, W. R.; Thomas, M. G.; Muetterties, E. L. *J. Am. Chem. Soc.* **1977**, *99*, 7380. (b) Muetterties, E. L.; Band, E.; Kokorin, A.; Pretzer, W. R.; Thomas, M. G. *Inorg. Chem.* **1980**, *19*, 1552.
(7) (a) Bradley, J. S. *J. Am. Chem. Soc.* **1979**, *101*, 7419. (b) Rathke, J. W.; Feder, H. M. *J. Am. Chem. Soc.* **1978**, *100*, 3623.
(8) For a recent review, see Dombek, B. D. *Adv. Catal.* **1983**, *32*, 325.
(9) (a) Thomas, M. G.; Beier, B. F.; Muetterties, E. L. *J. Am. Chem. Soc.* **1976**, *98*, 1296. (b) Demitras, G. C; Muetterties, E. L. *J. Am. Chem. Soc.* **1977**, *99*, 2796.
(10) (a) Manriquez, J. M.; McAlister, D. R.; Sanner, R. D.; Bercaw, J. E. *J. Am. Chem. Soc.* **1976**, *98*, 6733. (b) Manriquez, J. M.; McAlister, D. R.; Sanner, R. D.; Bercaw, J. E. *J. Am. Chem. Soc.* **1978**, *100*, 2716.
(11) Wolczanski, P. T.; Bercaw, J. E. *J. Am. Chem. Soc.* **1979**, *100*, 6450.
(12) Christian, D. F.; Clark, H. C.; Stepaniak, R. F. *J. Organomet. Chem.* **1976**, *112*, 209.
(13) Ciriano, M.; Green, M.; Gregson, D.; Howard, J. A. K.; Spencer, J. L.; Stone, F. G. A.; Woodward, P. *J. Chem. Soc., Dalton Trans.* **1979**, 1294.
(14) Alcock, N. W.; Brown, J. M.; MacLean, T. D. *J. Chem. Soc., Chem. Commun.* **1984**, 1689.
(15) Facchin, G.; Uguagliati, P.; Michelin, R. *Organometallics* **1984**, *3*, 1818.
(16) (a) Christian, D. F.; Clark, G. R.; Roper, W. R.; Waters, J. M.; Whittle, K. R. *J. Chem. Soc., Chem. Commun.* 1972, 458. (b) Christian, D. F.; Roper, W. R. *J. Organomet. Chem.* **1974**, *80*, C35. (c) Clark, G. R.; Waters, J. M.; Whittle, K. R. *J. Chem. Soc., Dalton Trans.* **1975**, 2556.
(17) Howell, J. A. S.; Mathur, P. *J. Chem. Soc., Chem. Commun.* **1981**, 263.
(18) Bruce, M. I.; Wallis, R. C. *Aust. J. Chem.* **1982**, *35*, 709.
(19) Adams, R. D.; Golembeski, N. M. *J. Am. Chem. Soc.* **1979**, *101*, 2579.
(20) (a) Andrews, M. A.; Kaesz, H. D. *J. Am. Chem. Soc.* **1979**, *101*, 7238. (b) Andrews, M. A.; van Buskirk, G.; Knobler, C. B.; Kaesz, H. D. *J. Am. Chem. Soc.* **1979**, *101*, 7245. (c) Andrews, M. A.; Kaesz, H. D. *J. Am. Chem. Soc.* **1979**, *101*, 7255. (d) Andrews, M. A.; Knobler, C. B.; Kaesz, H. D. *J. Am. Chem. Soc.* **1979**, *101*, 7260.
(21) Bernhardt, W.; Vahrenkamp, H. *Angew. Chem., Int. Ed. Engl.* **1984**, *23*, 381.
(22) Muetterties, E. L. *Bull. Soc. Chim. Belg.* **1976**, *85*, 451.
(23) Sivak, A. J.; Muetterties, E. L. *J. Am. Chem. Soc.* **1979**, *101*, 4878.
(24) McKenna, S. T.; Muetterties, E. L., submitted for publication.
(25) $R = (\sum||F_o| - |F_c||)/(\sum|F_o|)$, $R_w = \{[\sum w(|F_o| - |F_c|)^2]/[\sum wF_o^2]\}^{1/2}$, and GOF = $\{[\sum w(|F_o| - |F_c|)^2]/(n_o - n_v)\}^{1/2}$, where n_o is the number of observations and n_v is the number of variable parameters.

Table II. Positional Parameters for 2a, $(\mu\text{-H})(\mu\text{-4-ClC}_6H_4NMe)Rh_2[P(O\text{-}i\text{-PR})_3]_4$[a]

atom	x	y	z	B, Å²
Rh1	0.05363 (3)	0.20163 (3)	0.21460 (2)	3.68 (1)
Rh2	−0.08404 (3)	0.30952 (3)	0.21579 (2)	3.59 (1)
Cl	0.1119 (2)	0.3687 (2)	0.5047 (1)	11.36 (9)
P1	0.1294 (1)	0.1780 (1)	0.13110 (9)	4.88 (4)
P2	0.1244 (1)	0.12040 (9)	0.27116 (8)	4.34 (4)
P3	−0.2165 (1)	0.3476 (1)	0.25843 (8)	4.33 (4)
P4	−0.0856 (1)	0.3931 (1)	0.14979 (9)	4.9 (4)
O1	0.2050 (4)	0.1174 (3)	0.1317 (2)	6.8 (1)
O2	0.0647 (4)	0.1620 (5)	0.0725 (3)	11.4 (2)
O3	0.1915 (5)	0.2335 (3)	0.0955 (3)	11.8 (2)
O4	0.2369 (3)	0.1275 (3)	0.2862 (2)	5.6 (1)
O5	0.0805 (3)	0.1164 (3)	0.3380 (2)	5.5 (1)
O6	0.1305 (4)	0.0404 (2)	0.2529 (2)	6.1 (1)
O7	−0.2452 (3)	0.3032 (3)	0.3172 (2)	5.4 (1)
O8	−0.3146 (3)	0.3475 (2)	0.2188 (2)	5.2 (1)
O9	−0.2284 (3)	0.4255 (2)	0.2827 (2)	5.8 (1)
O10	−0.0414 (5)	0.3890 (3)	0.0856 (3)	11.0 (2)
O11	−0.1781 (4)	0.4390 (3)	0.1410 (3)	7.5 (1)
O12	−0.0189 (5)	0.4596 (3)	0.1710 (3)	9.8 (2)
N	−0.0461 (3)	0.2323 (3)	0.2807 (2)	3.9 (1)
C1	−0.0210 (4)	0.2629 (3)	0.3350 (3)	4.1 (1)
C2	0.0641 (5)	0.3088 (4)	0.3320 (3)	5.2 (2)
C3	0.106 (6)	0.3417 (4)	0.3840 (3)	6.3 (2)
C4	0.0638 (6)	0.3276 (5)	0.4395 (3)	6.8 (2)
C5	−0.0115 (6)	0.2842 (5)	0.4442 (3)	7.2 (2)
C6	−0.0487 (5)	0.2511 (4)	0.3922 (3)	5.7 (2)
C7	−0.1186 (5)	0.1766 (3)	0.2898 (3)	4.7 (2)
C11	0.2598 (6)	0.0960 (5)	0.0784 (4)	8.3 (2)
C12	0.236 (1)	0.0235 (6)	0.0641 (7)	17.1 (4)
C13	0.3629 (8)	0.1055 (8)	0.0931 (6)	14.9 (4)
C21	−0.0151 (8)	0.1263 (6)	0.0631 (4)	11.5 (3)
C22	−0.0966 (8)	0.121 (1)	0.0961 (5)	15.3 (6)
C23	−0.030 (1)	0.1145 (8)	−0.0039 (5)	15.5 (4)
C31	0.2112 (8)	0.3006 (5)	0.1054 (4)	9.3 (3)
C32	0.261 (1)	0.3256 (8)	0.0487 (6)	17.8 (5)
C33	0.2654 (8)	0.3199 (7)	0.1600 (6)	14.0 (4)
C41	0.2846 (5)	0.1928 (4)	0.2881 (4)	7.1 (2)
C42	0.3777 (7)	0.1868 (7)	0.2600 (6)	11.7 (4)
C43	0.2939 (8)	0.2172 (6)	0.3524 (5)	11.2 (3)
C51	0.1193 (6)	0.0777 (4)	0.3896 (4)	6.9 (2)
C52	0.078 (1)	0.0097 (6)	0.3936 (5)	12.7 (4)
C53	0.096 (1)	0.1170 (7)	0.4456 (5)	13.5 (4)
C61	0.00686 (6)	0.0057 (4)	0.2099 (4)	6.5 (2)
C62	0.1156 (8)	−0.0606 (5)	0.19652 (5)	11.1 (3)
C63	−0.0291 (7)	−0.0032 (6)	0.2347 (6)	10.9 (3)
C71	−0.3276 (6)	0.3171 (5)	0.3559 (4)	7.7 (2)
C72	−0.2961 (8)	0.3002 (9)	0.4186 (5)	15.9 (6)
C73	−0.4054 (7)	0.2756 (8)	0.3374 (5)	16.0 (4)
C81	−0.3294 (5)	0.3062 (4)	0.1653 (3)	5.7 (2)
C82	−0.4179 (8)	0.3326 (6)	0.1327 (5)	10.6 (3)
C83	−0.3392 (7)	0.2322 (5)	0.1798 (5)	9.9 (3)
C91	−0.1486 (6)	0.4624 (4)	0.3089 (4)	7.8 (2)
C92	−0.169 (1)	0.5373 (6)	0.3011 (7)	14.6 (5)
C93	−0.1307 (9)	0.4447 (7)	0.3731 (6)	13.9 (4)
C101	−0.0630 (8)	0.3258 (5)	0.0441 (4)	9.4 (3)
C102	0.000 (1)	0.3409 (8)	−0.0086 (5)	14.9 (5)
C103	−0.1596 (9)	0.315 (1)	0.0252 (6)	16.7 (6)
C111	−0.1847 (7)	0.5006 (5)	0.1001 (7)	13.9 (4)
C112	−0.280 (1)	0.5054 (8)	0.085 (1)	36.5 (7)
C113	−0.176 (2)	0.556 (1)	0.132 (1)	31.5 (8)
C121	0.0808 (6)	0.4556 (5)	0.1792 (5)	9.1 (3)
C122	0.1266 (7)	0.4966 (6)	0.1275 (5)	12.8 (3)
C123	0.1073 (8)	0.4813 (7)	0.2392 (6)	15.6 (4)

[a] Anisotropically refined atoms are given in the form of the isotropic equivalent thermal parameter defined as $(^4/_3)[a^2B(1,1) + b^2B(2,2) + c^2B(3,3) + ab(\cos\gamma)B(1,2) + ac(\cos\beta)B(1,3) + bc(\cos\alpha)B(2,3)]$. Anisotropic thermal parameters and hydrogen atom positions are given in the supplementary material.

complexes **2a,b** (Scheme II). Spectroscopic and microanalytical data are consistent with the formulation of **2** as $(\mu\text{-H})(\mu\text{-RNMe})Rh_2[P(O\text{-}i\text{-Pr})_3]_4$. Thus the infrared spectra show no evidence of C–N multiple bond or N–H stretching modes. The ^1H NMR spectrum shows a single hydride resonance split into a triplet ($J_{HP(trans)} \approx 85$ Hz)

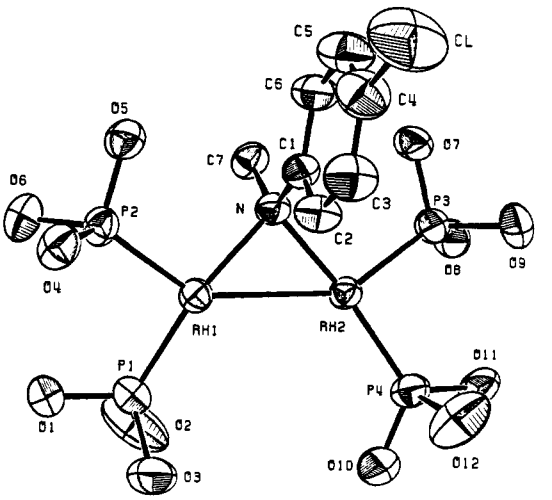

Figure 1. ORTEP diagram of **2a**. For clarity, the isopropyl groups on the phosphite ligands have been omitted.

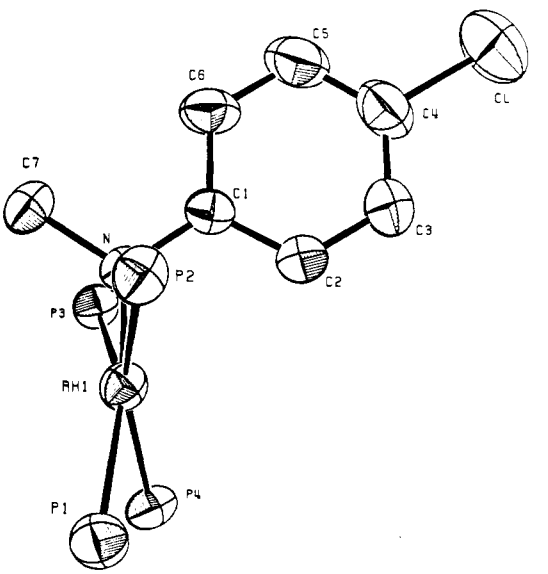

Figure 2. View of **2a** looking directly down the Rh_1–Rh_2 vector. The isopropoxide groups on the phosphites have been omitted for clarity.

of triplets ($J_{HRh} \approx 21$ Hz) of triplets ($J_{HP(cis)} \approx 10$ Hz); this assignment was confirmed by broad-band ^{31}P decoupling. The N-bound methyl group appears as a broad singlet with barely resolvable quintet structure ($J_{HP} \approx 4$ Hz) which becomes a sharp singlet upon ^{31}P decoupling. The pattern of the phosphite isopropyl resonances is diagnostic; two different methine resonances are observed, corresponding to the two different phosphite environments in the structure in Scheme II, but there are four resonances for the phosphite methyls. This is because the presence of two different organic groups bound to the tetrahedrally coordinated amido nitrogen destroys the mirror symmetry of the Rh_2P_4 plane, so the methyl groups on a given phosphite isopropyl are diastereotopic and give different NMR signals. The same features are observed in the $^{13}C\{^1H\}$ NMR as well, and a quartet in the ^1H-coupled ^{13}C spectrum confirms the assignment of the NMe group. The $^{31}P\{^1H\}$ NMR spectrum shows the AA′BB′ part of an AA′BB′XX′ pattern, as expected (vide infra).

In order to characterize these compounds more fully, the X-ray crystal structure of **2a** was obtained. Table I lists the crystal and data collection parameters; Tables II through IV give the atomic coordinates, bond lengths, and bond angles, respectively. Perspective views of the mol-

Table III. Intramolecular Distances (Å) for 2a

atom 1	atom 2	distance	atom 1	atom 2	distance
Rh1	Rh2	2.844 (1)	O5	C51	1.449 (7)
Rh1	P1	2.178 (2)	O6	C61	1.429 (7)
Rh1	P2	2.221 (1)	O7	C71	1.469 (7)
Rh2	P3	2.216 (1)	O8	C81	1.429 (7)
Rh2	P4	2.171 (2)	O9	C91	1.432 (8)
Rh1	N	2.114 (4)	O10	C101	1.552 (10)
Rh2	N	2.122 (4)	O11	C111	1.495 (14)
N	C1	1.399 (6)	O12	C121	1.401 (9)
N	C7	1.498 (6)	C11	C12	1.477 (13)
C1	C2	1.390 (7)	C11	C13	1.479 (13)
C2	C3	1.390 (8)	C21	C22	1.366 (12)
C3	C4	1.354 (9)	C21	C23	1.491 (11)
C4	C5	1.353 (9)	C31	C32	1.514 (12)
C5	C6	1.396 (9)	C31	C33	1.447 (14)
C6	C1	1.379 (7)	C41	C42	1.454 (11)
CL	C4	1.753 (7)	C41	C43	1.484 (12)
P1	O1	1.580 (4)	C51	C52	1.445 (11)
P1	O2	1.579 (5)	C51	C53	1.482 (11)
P1	O3	1.597 (5)	C61	C62	1.479 (10)
P2	O4	1.602 (4)	C61	C63	1.490 (10)
P2	O5	1.598 (4)	C71	C72	1.463 (12)
P2	O6	1.607 (4)	C71	C73	1.403 (11)
P3	O7	1.604 (4)	C81	C82	1.501 (9)
P3	O8	1.602 (4)	C81	C83	1.479 (10)
P3	O9	1.615 (4)	C91	C92	1.491 (12)
P4	O10	1.546 (5)	C91	C93	1.459 (12)
P4	O11	1.576 (4)	C101	C103	1.420 (13)
P4	O12	1.653 (6)	C111	C112	1.370 (17)
O1	C11	1.468 (7)	C111	C113	1.29 (3)
O2	C21	1.324 (9)	C121	C122	1.534 (12)
O3	C31	1.348 (10)	C121	C123	1.443 (14)
O4	C41	1.434 (8)			

ecule are shown in Figures 1 and 2. The geometry at each Rh is roughly square-planar, and the amido and hydride (not located but presumably trans to P_2 and P_3) ligands bridge the two rhodium centers. the Rh–Rh distance of 2.844 (1) Å is similar to other $(\mu\text{-H})(\mu\text{-X})Rh_2[P(O\text{-}i\text{-}Pr)_3]_4$ compounds (X = RC=CHR, 2.936 (1) and 2.889 (2) Å;[3b] X = Cl, 2.892 (1) Å[26]) and considerably shorter than the nonbonding distance of $(\mu\text{-X})_2Rh_2L_4$ complexes (e.g., X = Cl, L = $P(O\text{-}i\text{-}Pr)_3$, 3.431 Å[26]). The bond angles about the rhodiums are somewhat distorted from ideality due to the large size of the phosphite ligands; the cis P–Rh–P and P–Rh–N angles range from 91.9° to 98.8°, while the trans P–Rh–N angles (both about 166.2°) show that P_1 and P_4 are displaced toward the relatively empty space near the hydride. The P–Rh distances trans to the hydride (2.221 (1) and 2.216 (1) Å) are significantly longer than those trans to the nitrogen (2.178 (2) and 2.171 (2) Å), consistent with a stronger trans influence for the hydride than for the amido ligand. Due to the larger radius of the nitrogen compared to the hydride (Rh–N = 2.114 (4) and 2.122 (4) Å here vs. roughly 1.7–1.8 Å for Rh–H in similar compounds[3b,27,28]) the joining of the two square planes is not symmetrical. Thus the angles Rh–Rh–$P_{2,3}$ average 145°, and these Rh–P bonds are essentially opposed across the Rh–Rh vector, while the bonds to P_1 and P_4 are closer to parallel, having Rh–Rh–$P_{1,4}$ angles averaging 122°. This is observable in the $^{31}P\{^1H\}$ NMR as well (vide infra).

The bridging arylmethylamido group is roughly tetrahedral (Rh–N–C and C–N–C angles ranging from 109.8° to 118.7°) except for the small Rh_1–N–Rh_2 angle (84.3 (1)°) enforced by the Rh–Rh bond. The aromatic ring lies nearly perpendicular to the Rh–Rh vector in the plane

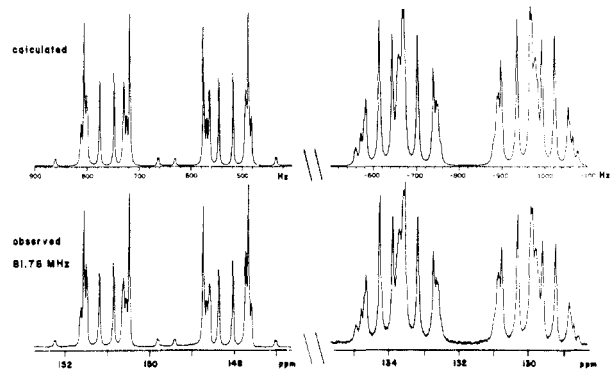

Figure 3. Observed and calculated $^{31}P\{^1H\}$NMR spectra of **2b**. The downfield portion is due to P_B; the upfield portion is due to P_A. The vertical scale of P_A has been increased by a factor of 3. The horizontal scale of the calculated spectrum is in hertz relative to an arbitrary origin.

between the two RhPP groups. The molecule is twisted slightly about the Rh–Rh axis (see Figure 2); the two RhPP planes have a 24.0° dihedral angle, and the Rh_1Rh_2N plane lies unsymmetrically between them, 8.8° from the $Rh_1P_1P_2$ plane and 15.3° from RhP_3P_4. The twist is presumably due to steric and crystal packing effects and is not observed in a static sense in solution.

The $^{31}P\{^1H\}$ NMR spectra of the complexes **2** suggest that the solid-state structure is maintained in solution. Since all the rhodium and phosphorus nuclei are magnetically inequivalent, the spin system is AA'BB'XX' and the resulting spectra are quite complicated. Simulations reproduce the spectra accurately (Figure 3) and enable the determination of all coupling constants as well as the relative signs of all but the Rh–Rh coupling constant (Table V). A number of interesting features can be seen. Consistent with the fact that P_2 and P_3 (A and A') are nearly opposed across the Rh–Rh vector, the four-bond P–P coupling $J_{AA'}$ is very large, larger in fact than the two-bond coupling J_{AB}. The other four-bond couplings, $J_{AB'}$ and $J_{BB'}$, are very small. For the same reason, the three-bond coupling between $P_{2,3}$ and the distant Rh ($J_{AX'}$) is larger than the analogous coupling for $P_{1,4}$ ($J_{BX'}$). Interestingly, the trans influence seen in the one-bond P–Rh coupling constants is opposite that seen in the crystal structure; $^1J_{AX}$ (trans to hydride) is much larger than $^1J_{BX}$ (trans to N). This is opposite the trend seen in mononuclear Pt complexes.[29] Due to the rarity of late transition-metal amido complexes,[30] however, the generality of this observation is unclear.

The aromatic ring in **2a** lies in the idealized mirror plane of the molecule, sandwiched between the isoproxide groups of phosphites on each side. In this orientation, all four protons on the ring have distinct chemical environments. Rotation of the ring about the C_1–N bond averages the four environments into two groups of two, ortho and meta to the C_1–N bond. Consistent with this, the 200-MHz ^1H NMR spectrum of **2a** at −50 °C has four separate aromatic resonances (δ 7.34 and 6.84 ortho, δ 6.92 and 6.59 meta). The spectrum is broad from −30 °C to above room temperature and reassembles as two resonances (δ 7.15 and 6.73) at 45 °C. Coalescence is at −15 °C. With use of a

(26) DelPaggio, A. A.; Muetterties, E. L.; Day, V. W.; Day, C. S.; Andersen, R. A., manuscript in preparation.
(27) Brown, R. K.; Williams, J. M.; Sivak, A. J.; Muetterties, E. L. *Inorg. Chem.* **1980**, *19*, 370.
(28) Teller, R. G.; Williams, J. M.; Koetzle, T. F.; Burch, R. R.; Gavin, R. M.; Muetterties, E. L. *Inorg. Chem.* **1981**, *20*, 1806.
(29) Pidcock, A. In *Catalytic Aspects of Metal Phosphine Complexes*; Alyea, E. C., Meek, D. W., Eds.; Advances in Chemistry 196, American Chemical Society: Washington, DC, 1982; p 1.
(30) (a) Lappert, M. F.; Power, P. P.; Sanger, A. R.; Srivastava, R. C. *Metal and Metalloid Amides*; Ellis Horwood: Chichester, U.K., 1980. (b) Eadie, D. T.; Pidcock, A.; Stobart, S.; Brennan, E.; Cameron, T. S. *Inorg. Chim. Acta* **1982**, *65*, L111. (c) Bryndza, H. E.; Fultz, W. C.; Tam, W. *Organometallics* **1985**, *4*, 939.

Table IV. Intramolecular Angles (deg) for 2a

atom 1	atom 2	atom 3	angle	atom 1	atom 2	atom 3	angle
Rh2	Rh1	P1	120.32 (5)	P2	O6	C61	125.7 (4)
Rh2	Rh1	P2	144.14 (4)	P3	O7	C71	125.2 (4)
Rh1	Rh2	P3	145.10 (4)	P3	O8	C81	123.1 (3)
Rh1	Rh2	P4	122.80 (4)	P3	O9	C91	121.0 (4)
Rh2	Rh1	N	47.95 (11)	P4	O10	C101	119.6 (5)
Rh1	Rh2	N	47.71 (10)	P4	O11	C111	124.4 (5)
P1	Rh1	P2	95.54 (6)	P4	O12	C121	122.9 (5)
P3	Rh2	P4	91.92 (6)	O1	C11	C12	108.6 (7)
P1	Rh1	N	166.24 (12)	O1	C11	C13	108.3 (7)
P2	Rh1	N	96.45 (11)	O2	C21	C22	132.0 (9)
P3	Rh2	N	98.79 (11)	O2	C21	C23	109.4 (8)
P4	Rh2	N	166.07 (11)	O3	C31	C32	106.0 (8)
Rh1	N	Rh2	84.34 (14)	O3	C31	C33	118.9 (9)
Rh1	N	C1	118.7 (3)	O4	C41	C42	109.7 (7)
Rh1	N	C7	110.2 (3)	O4	C41	C43	109.9 (6)
Rh2	N	C1	109.8 (3)	O5	C51	C52	112.4 (7)
Rh2	N	C7	116.2 (3)	O5	C51	C53	106.9 (6)
C1	N	C7	114.3 (4)	O6	C61	C62	106.2 (6)
C2	C1	C6	116.8 (5)	O6	C61	C63	111.1 (6)
C1	C2	C_3	121.5 (5)	O7	C71	C72	105.9 (6)
C2	C3	C4	119.8 (6)	O7	C71	C73	109.9 (7)
CL	C4	C3	119.2 (6)	O8	C81	C82	107.3 (6)
CL	C4	C5	120.3 (6)	O8	C81	C83	112.6 (6)
C3	C4	C_5	120.5 (6)	O9	C91	C92	107.3 (7)
C4	C5	C6	120.0 (6)	O9	C91	C93	112.2 (8)
C1	C6	C5	121.3 (6)	O10	C101	C102	100.6 (9)
Rh1	P1	O1	119.20 (17)	O10	C101	C103	117.1 (9)
Rh1	P1	O2	116.08 (20)	O11	C111	C112	104.0 (11)
Rh1	P1	O3	122.99 (22)	O11	C111	C113	109.6 (18)
Rh1	P2	O4	118.30 (16)	O12	C121	C122	107.9 (9)
Rh1	P2	O5	111.48 (15)	O12	C121	C123	109.2 (8)
Rh1	P2	O6	125.10 (17)	C12	C11	C13	112.1 (9)
Rh2	P3	O7	112.54 (15)	C22	C21	C23	113.7 (9)
Rh2	P3	O8	118.98 (15)	C32	C31	C33	110.4 (10)
Rh2	P3	O9	122.96 (16)	C42	C41	C43	111.4 (7)
Rh2	P4	O10	124.38 (21)	C52	C51	C53	109.0 (8)
Rh2	P4	O11	119.95 (16)	C62	C61	C63	112.7 (7)
Rh2	P4	O12	113.69 (20)	C72	C71	C73	110.8 (9)
P1	O1	C11	124.4 (4)	C82	C81	C83	110.9 (6)
P1	O2	C21	133.7 (6)	C92	C91	C93	111.6 (8)
P1	O3	C31	133.3 (5)	C102	C101	C103	112.4 (9)
P2	O4	C41	122.3 (4)	C112	C111	C113	98.8 (16)
P2	O5	C51	126.1 (4)	C122	C121	C123	112.7 (7)

Table V. $^{31}P\{^1H\}$ NMR for $(\mu\text{-}H)(\mu\text{-}RNMe)Rh_2[P(O\text{-}i\text{-}Pr)_3]_4$

parameter[a]	R = 4-ClC_6H_4, **2a**	R = $PhCH_2$, **2b**
δ_A	132.74	131.70
δ_B	149.73	149.59
$^1J_{AX}$	297.8[b]	311.9[b]
$^3J_{AX'}$	+7.8	+9.1
$^1J_{BX}$	+247.8	+232.8
$^3J_{BX'}$	−3.6	−3.3
$^2J_{AB}$	+82.5	+80.8
$^4J_{AB'}$	+6.2	+6.8
$^4J_{AA'}$	+85.6	+84.7
$^4J_{BB'}$	−6.0	−1.3
$^2J_{XX'}$	3.0	5.7

[a] For labeling scheme, see text. J values in hertz. [b] Where provided, signs are determined and are given relative to $J_{AX'}$, assumed positive.

simple coalescence temperature approximation,[31] this gives $\Delta G^{\ddagger}$ = 12.0 kcal/mol at −15 °C for the hindered rotation about the C_1–N bond.

Evidence for a Formimidoyl Intermediate. The overall conversion from **1** to **2** must involve the oxidative addition of H_2 and three hydrogen transfers to the isocyanide carbon to generate the NMe group. The first hydrogen transfer should yield a formimidoyl species, $H_x(RN{=}CH)Rh_2[P(O\text{-}i\text{-}Pr)_3]_4$. A key question is when in the sequence H_2 addition occurs, i.e., before or after the first (or second) hydrogen transfer (see Scheme III).

Scheme III. Possible Pathways for the Reaction of 1 with Hydrogen[a]

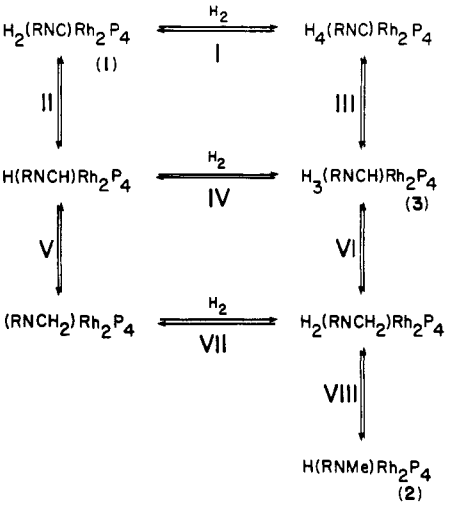

[a] Only the numbered species have been observed.

A clue to this is obtained by NMR monitoring of the reaction of **1a,b** with hydrogen. Within a few hours (1 atm of H_2, 20 °C), a new species, **3a,b**, appears. This species is tentatively identified as the formimidoyl complex H(μ-

(31) Sandstrom, J. *Dynamic NMR Spectroscopy*; Academic Press: New York, 1982.

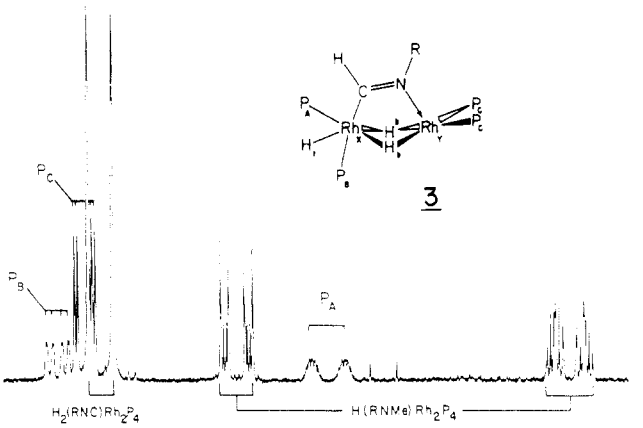

Figure 4. $^{31}P\{^1H\}$NMR spectrum taken during the reaction of **1a** with H_2, showing **1a**, **2a**, and **3a** (structure in inset).

$H)_2(RN{=}CH)Rh_2[P(O\text{-}i\text{-}Pr)_3]_4$, with a structure like that shown in Figure 4, for the following reasons. A downfield resonance in the ^1H NMR (δ 10.10 for **3a**) with coupling to two distinct ^{31}P nuclei is due to the unique formimidoyl proton. There are two hydride signals in a 2:1 ratio, both complex multiplets; in the $^1H\{^{31}P\}$ NMR spectrum, they become a triplet and a doublet, respectively ($^1J_{HRh} \approx 18$ Hz for both), indicating two bridging hydrides and one terminal hydride. There are four distinct signals of equal intensity for the phosphite methyl protons. The $^{31}P\{^1H\}$ NMR spectrum of **3a** is shown in Figure 4 (recorded during the reaction and therefore showing **1a** and **2a** as well). It consists of a doublet of doublets with intensity 2 due to P_C, split by Rh_Y (185 Hz) and P_A (34 Hz); a doublet of doublets of multiplets due to P_B, split by Rh_X (164 Hz), P_A (64 Hz), plus Rh_Y, and possibly P_C; and a doublet of multiplets for P_A, split by Rh_X (338 Hz) and the other nuclei.

The structure proposed for the formimidoyl intermediate in Figure 4 is very similar to that of $H(\mu\text{-}H)_3Rh_2[P(O\text{-}i\text{-}Pr)_3]_4$,[32] differing only in the replacement of the unique bridging hydride by a formimidoyl ligand. Thus, like $H(\mu\text{-}H)_3Rh_2[P(O\text{-}i\text{-}Pr)_3]_4$, it is formally mixed-valence, with Rh_X in the +3 oxidation state and Rh_Y in the +1 state. The formimidoyl is shown with the nitrogen bound through its lone pair to Rh_Y; although geometric constraints can allow it to be within bonding distance of Rh_Y, there is no indication in the ^1H or $^{31}P\{^1H\}$ NMR for or against such an interaction,[33] nor can side-on (π) bonding to Rh_Y be ruled out. The geometry at Rh_X, in particular the disposition of P_A and the terminal hydride, is unclear and has been left unspecified in Figure 4. The NMR data at the temperatures studied (as low as −50 °C) require C_s symmetry; an effective mirror plane contains Rh_X, Rh_Y, P_A, P_B, the terminal hydride, and the formimidoyl ligand and relates the two bridging hydrides and the P_C's. This can be seen for several reasons. The two P_C's have the same ^{31}P chemical shift and coupling constants; the bridging hydrides are likewise equivalent in the ^1H NMR. Furthermore, there are four phosphite methyl resonance in a 1:1:1:1 ratio in the 500-MHz ^1H NMR spectrum, due to P_A, P_B, and the two diasteriotopic types of methyls on the P_C's. If there were no mirror plane containing P_A and P_B, their isopropyl groups would have diasteriotopic methyls as well, and there would be eight methyl signals in all. Thus in at least a time-averaged sense, P_A, P_B, the terminal hydride, and the formimidoyl ligand on Rh_X all lie in the same plane. A plausible explanation is that the geometry at Rh_X is roughly octahedral, with the formimidoyl ligand and P_B mutually trans and with P_A and H_t exchanging places with one another in a rapid fluxional process. Equivalently, this may be viewed as saying that Rh_X is coordinated in a trigonal-bipyramidal fashion, with the formimidoyl ligand and P_B axial and the bridging hydrides and P_A equatorial and that the terminal hydride jumps from face to face of the polyhedron, giving an effective mirror plane. In either case, the terminal hydride does not exchange with the bridging hydrides. Note that the same effective mirror symmetry and fluxional behavior is observed for the isostructural compound $H(\mu\text{-}H)_3Rh_2[P(O\text{-}i\text{-}Pr)_3]_4$.[23]

The question of the timing of the first insertion is addressed by the reaction of **1** with D_2 rather than H_2. When this reaction is followed by $^2H\{^1H\}$ NMR, the deuteride resonance of the starting material **1** grows in rapidly (within ca. 30 min) as deuterium exchanges into the hydride position and then disappears slowly (>3 times slower than H/D exchange) as **1** is converted to **3**. This requires that the oxidative addition of hydrogen or deuterium (e.g., steps I or IV in Scheme III) must be reversible and that the process of oxidative addition followed by reductive elimination must be capable of scrambling deuterium into all hydride sites. If insertion preceds the oxidation addition (i.e., path II/IV in Scheme III), then this step must be reversible as well. Both of the equilibria I and II must lie far toward complex **1**, since no evidence of insertion products is seen in the absence of hydrogen, and the addition of RNC to $H(\mu\text{-}\leq H)_3Rh_2[P(O\text{-}i\text{-}Pr)_3]_4$ under hydrogen gives **1** quantitatively (by NMR); low-temperature NMR (to −80 °C) failed to detect any species other than **1**, **2**, and **3**. The kinetic data available are insufficiently precise to distinguish between paths I/III and II/IV. However, it should be noted that equilibrium II would proceed in the absence of hydrogen as well. Since the thermal decomposition (20 °C, 2–3 days) of **1** shows no products identifiable as resulting from insertion reactions, reaction path II/IV seems less likely than I/III.

No species resulting from a second insertion (such as $H_2(RNCH_2)Rh_2P_4$) are observed by NMR. This and the fact that **3** builds up in the reaction mixture indicate that the second insertion (step VI in Scheme III) is relatively slow, while the third (step VIII) must be faster. Since the slow step involves the formation of a C–H bond at the expense of a Rh–H bond, an inverse kinetic isotope effect might be expected.[34] Our data does suggest $k_D/k_H = 2\text{–}4$ for formation of **2a**.[35] Similar values are obtained for the disappearance of **1a** and **3a**. All three measurements are of limited precision due to overlapping resonances, however, and it is likely that k_H and k_D are composites of several rate constants.

Further Hydrogenation. Upon further reaction of **2a,b** (either previously isolated or prepared in situ from **1**) with hydrogen, a slow color change to red is observed. The red product has been identified as $H(\mu\text{-}H)_3Rh_2[P(O\text{-}i\text{-}Pr)_3]_4$ by NMR and by isolation of $(\mu\text{-}H)_2Rh_2[P(O\text{-}i\text{-}Pr)_3]_4$ after removal of H_2. Analysis of the volatile components of the reaction mixture by GC and GC/MS revealed an equivalent amount of the secondary amines RNHMe (R

(32) Meier, E.-B.; Burch, R. R.; Muetterties, E. L.; Day, V. W. *J. Am. Chem. Soc.* **1982**, *104*, 2661.

(33) The ^{103}Rh NMR spectrum of **3a** has been recorded, however; the chemical shift of Rh_Y is suggestive, but not conclusive, of a bound nitrogen. McKenna, S. T.; Andersen, R. A.; Muetterties, E. L., manuscript in preparation.

(34) Wiberg, K. B. *Chem. Rev.* **1955**, *55*, 713.

(35) A value of $k_D/k_H = 2.5$ has been found for an olefin hydrogenation reaction: Howarth, O. W.; McAteer, C. H.; Moore, P.; Morris, G. E. *J. Chem. Soc., Chem. Commun.* **1982**, 745.

Scheme IV. Overall Cycle for the Hydrogenation of Isocyanides Mediated by $(\mu\text{-H})_2Rh_2[P(o\text{-}i\text{-}Pr)_3]_4$

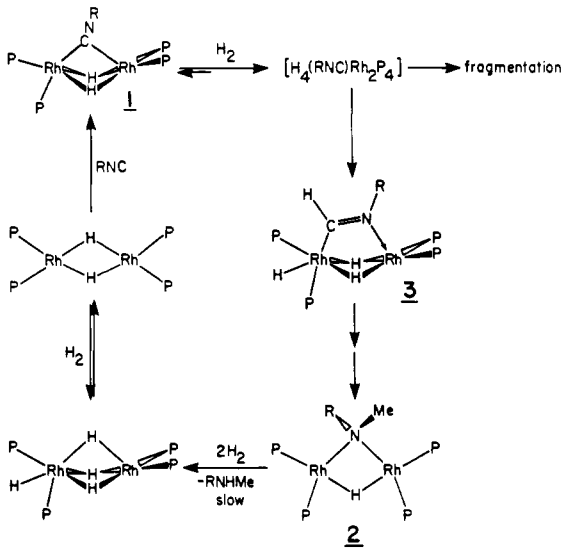

= 4-ClC_6H_4, $PhCH_2$), the result of complete hydrogenation of the original isocyanides. The reaction is extremely slow, however, giving only about 10% conversion (based on $(\mu\text{-H})_2Rh_2[P(O\text{-}i\text{-}Pr)_3]_4$; see Experimental Section) in 10–15 days under 1–2 atm of hydrogen, and has not been carried out to completion. This reaction appears to be due to hydrogenolysis of **2** rather than hydrolysis by adventitious water, since **2b** was found to be only slightly reactive toward 3 equiv of H_2O, giving after 7 days only an 8% conversion to $(\mu\text{-H})(\mu\text{-OH})Rh_2[P(O\text{-}i\text{-}Pr)_3]_4$;[36] the latter compound does not convert to $H(\mu\text{-H})_3Rh_2[P(O\text{-}i\text{-}Pr)_3]_4$ on reaction with hydrogen. The hydrogenolysis of **2** thus completes a cycle for the stoichiometric hydrogenation of isocyanides to secondary amines, although with an extremely slow final step (Scheme IV). The reaction is unfortunately not useful in a catalytic sense, since both **1** and **2** are highly reactive toward additional isocyanide (vide infra).

H/D Exchange. In the reaction of **1a,b** with D_2, deuterium NMR shows the appearance of D in the expected places: the hydrides of **2** and **3**, the formimidoyl position of **3**, and the *N*-methyl position of **2**. However, it also appears in an unexpeected place, the phosphite methyl groups. Figure 5 shows $^2H\{^1H\}$ NMR spectra obtained during the reaction of **1a** with D_2. After 4.5 h, **1a** is nearly gone, but resonances for **2a** and **3a** are visible; a set of resonances for the four phosphite methyl peaks of **2a** can already be seen. At 27 h, the formation of **2a** has gone to completion. The integral ratio of the NCD_3 group to the bridging deuteride is 3:0.9 and the phosphite methyl region integrates as 1.3 D's. After 10 days (in a sealed system) the NCD_3 to deuteride ratio is 3:0.4, and the phosphite methyl region is now over 11 D's vs. the NCD_3 group. Similarly, when all-protio **2a** is allowed to equilibrate under 2 atm of D_2 at room temperature for 9 days, its $^2H\{^1H\}$ NMR spectrum shows extensive D incorporation at the hydride and phosphite methyl positions. Deuterium appears about equally in the four phosphite methyl positions, and the integral of phosphite methyl vs. deuteride is 25:1. No signal is observed for the *N*-methyl group, showing that this group is stable toward H/D exchange. There is no D incorporation into the phosphite methine positions or

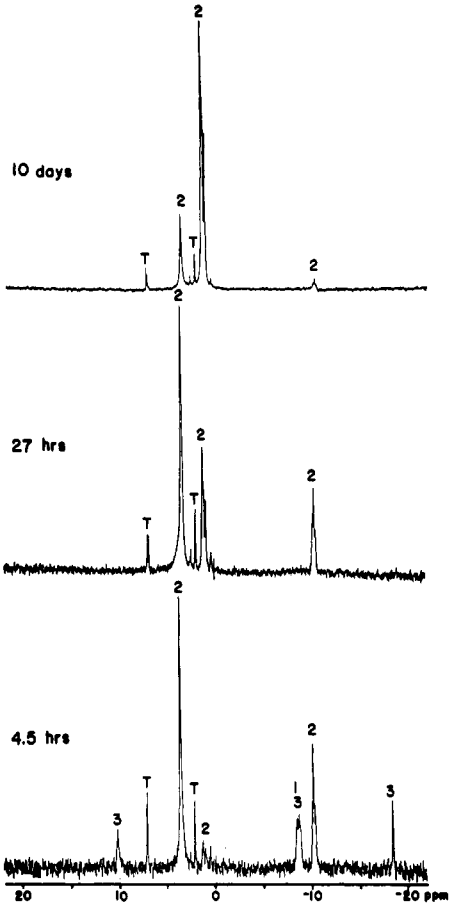

Figure 5. Deuterium NMR spectra taken during the reaction of **1a** with D_2. Numbers identify the species (**1a**, **2a**, or **3a**) responsible for each resonance; "T" marks resonances due to natural-abundance deuterium in the solvent (toluene). Vertical scale decreases from bottom spectrum to top (note toluene resonances for relative scale).

into the aromatic positions. The benzyl analogue **2b** shows similar behavior, except that deuterium also appears in the benzylic and ortho (but not meta or para) aromatic positions.

The selectivity of the H/D exchange suggests that it is an intramolecular process rather than an intermolecular (or heterogeneous, e.g., catalyzed by Rh metal) one. While the lack of attack on the phosphite methine positions could conceivably be due to steric hindrance, this does not explain the complete selectivity for the ortho over the meta and para positions of the benzyl group; in an intermolecular process, the meta and para positions should be attacked preferentially, in fact, due to their accessibility. While intramolecular H/D exchange in transition metal complexes is common with aromatic ligands, it is less frequent in saturated positions.[37] A common feature observed is that H/D exchange is most facile at positions four bonds removed from the metal center, such that binding of the metal to the affected position would form a relatively unstrained five-membered ring. Thus in deuteration of $PPh_2(OPh)$ with D_2 catalyzed by $RuHCl(PPh_3)_3$, the phenoxide ortho positions were deuterated 50 times faster than those of the other phenyls.[37] Similarly, Masters[38] observed specific deuteration at the methyl groups in $Pt_2Cl_4P_2$ (P = P-*n*-Pr_3) or at the C-3 position of the P-*n*-Bu_3 compound upon heating in CH_3COOD/D_2O.

(36) DelPaggio, A. A.; McKenna, S. T.; Burch, R. R.; Muetterties, E. L.; Day, V. W., unpublished results. We are grateful to Prof. M. D. Fryzuk for helpful discussions concerning this and similar compounds.

(37) Parshall, G. W. *Acc. Chem. Res.* **1970**, *3*, 139; **1975**, *8*, 113 and references therein.

(38) Masters, C. *J. Chem. Soc., Chem. Commun.* **1973**, 191.

Scheme V. Proposed Mechanism for the Exchange of the Phosphite Methyl Protons of 2a with D_2[a]

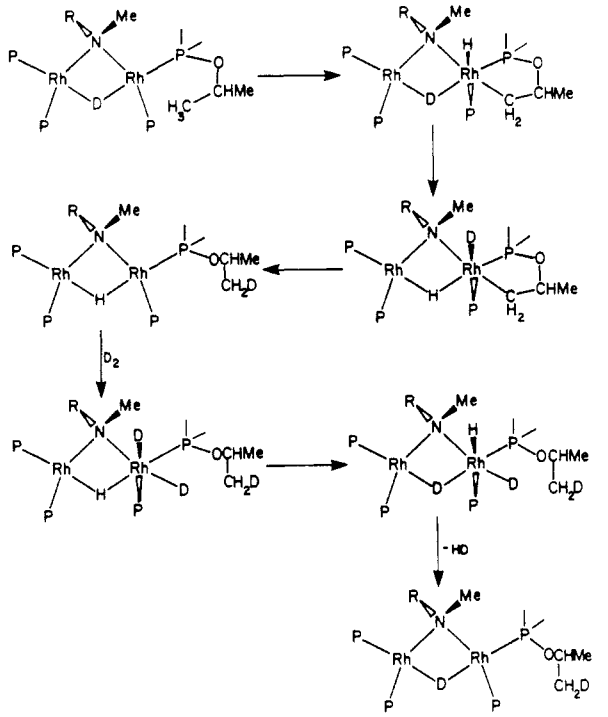

[a] Exchange is shown for only one type of phosphite; a similar mechanism operates on the other phosphite environment.

In a recent example, Caulton and co-workers[39a] found D incorporation into the C-3 positions (and, more slowly, into the C-2 positions) of the cyclohexyl groups of $H_7Re(PCy_3)_2$ upon heating in C_6D_6.

Scheme V shows a mechanism similar to that of Parshall[37] for the H/D exchange process. The methyl C–H bonds on the phosphite ligands can oxidatively add to the nearby Rh to give a five-membered metallacycle. The resulting hydride exchanges with the bridging deuteride and upon reductive elimination the deuterium is incorporated into the isopropoxide at the methyl position. Deuterium is returned to the hydride position by a similar reaction with D_2 gas, releasing HD. Deuterium accumulates in the methyls rather than the hydride positions for two reasons: their statistical advantage (72 methyl positions vs. 1 hydride), and the thermodynamic isotope effect (the total zero-point vibrational energy is lower with D bound to C and H bound to Rh than vice versa). Thus, in a closed system, the phosphite methyls, the hydride, and the gaseous $H_2/HD/D_2$ will behave as a single pool, and D will be preferentially stripped out of the hydride position to accumulate in the phosphite methyls, as seen in Figure 5. The phosphite methines are not attacked because to do so would generate a strained four-membered metallacycle. In **2b**, attack on the ortho position of the benzyl group generates a five-membered metallacycle and exchange occurs readily here. Oxidative addition of a benzylic C–H bond, however, gives a three-membered ring; the fact that exchange occurs here at all is probably a reflection of the low benzylic C–H bond strength.[40]

There is nothing in the mechanism of Scheme V which is necessarily specific to the complexes **2**. The mechanism should be equally applicable to any compounds in this system containing vacant coordination sites. In fact, we have observed the same process in the parent compound $(\mu\text{-H})_2Rh_2[P(O\text{-}i\text{-}Pr)_3]_4$. After equilibration with deuterium gas (700 torr) for 3 days, the recovered $(\mu\text{-D})_2Rh_2[P(O\text{-}i\text{-}Pr)_3]_4$, in addition to being quantitatively exchanged at the hydride position, contains approximately 2 D's in the phosphite methyls; no exchange is seen at the methine position.

Scheme VI. Routes to Ligand-Substituted Derivatives of 2

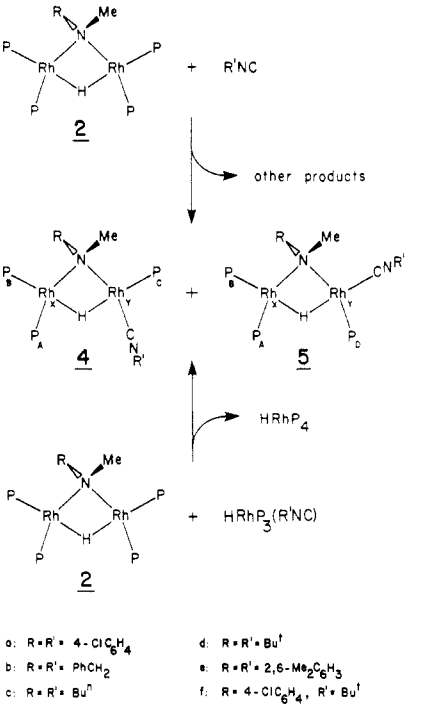

Substitution and Fragmentation Reactions. The addition of 1 equiv of $4\text{-}ClC_6H_4NC$ to **2a** results in rapid reaction to give a reddish brown solution from which it proved impossible to isolate any new products. By NMR spectroscopy, it was shown to contain a large number of compounds, including $HRh[P(O\text{-}i\text{-}Pr)_3]_3(RNC)$, $HRh[P(O\text{-}i\text{-}Pr)_3]_4$, $(\mu\text{-RNC})_2Rh_2[P(O\text{-}i\text{-}Pr)_3]_4$, and unreacted **2a**, but the major product (~45%) was a new compound containing two distinct rhodiums, three distinct phosphites, a coordinated isocyanide, an RNMe group, and one bridging hydride. A likely explanation is a substitution compound formed by replacing one phosphite of **2a** by R′NC (Scheme VI). The resulting compound $(\mu\text{-H})(\mu\text{-RNMe})Rh_2[P(O\text{-}i\text{-}Pr)_3]_3(R'NC)$ can have two isomers, one with the isocyanide cis to the hydride (**4**) and one with the isocyanide trans (**5**). The NMR data for the compound formed in the reaction of **2a** with $4\text{-}ClC_6H_4NC$, particularly the observation of two trans and one cis phosphorus couplings to the hydride, identified it as **4a**. No **5a** is observed.

The direct reaction of **2a** with isocyanide produced too many side products to be of use. A milder source of isocyanide, which would generate only minute quantities of free isocyanide at a time, should give cleaner results. Such a source is $HRh[P(O\text{-}i\text{-}Pr)_3]_3(RNC)$, which would release isocyanide only slowly (if at all; no dissociation is obvious by NMR) to give the stable complex $HRh[P(O\text{-}i\text{-}Pr)_3]_3$;[41] the phosphite displaced in the substitution would be trapped by the $HRh[P(O\text{-}i\text{-}Pr)_3]_3$ to form $HRh[P(O\text{-}i\text{-}Pr)_3]_4$ (Scheme VI). This method was found to work quite cleanly, although slowly. The reaction of **2a** with $HRh[P(O\text{-}i\text{-}Pr)_3]_3(t\text{-BuNC})$ reaches an apparent equilibrium

(39) For recent examples: (a) Zeiher, E. H. K.; DeWitt, D. G.; Caulton, K. G. *J. Am. Chem. Soc.* **1984**, *106*, 7006. (b) Chaudret, B. *J. Organomet. Chem.* **1984**, *268*, C33.

(40) Streitwieser, A.; Heathcock, C. H. *Introduction to Organic Chemistry*; Macmillan: New York, 1976.

(41) McKenna, S. T.; Muetterties, E. L.; Andersen, R. A., manuscript in preparation.

after about 8 days at room temperature to give a roughly 7:1 mixture of **4f** and **5f** along with $HRh[P(O\text{-}i\text{-}Pr)_3]_4$ and some unreacted starting materials. The equilibrium ratio **[4f + 5f]** $[HRhP_4]/$**[2a]**$[HRhP_3(R'NC)]$ was found to be about 20 in this case (based on only one measurement).

As mentioned previously, the hydrogenation of **1a,b** gives mainly **2a,b**. The yield of **2a** was found to be about 90%. The remainder was mostly $(\mu\text{-H})_2Rh_2[P(O\text{-}i\text{-}Pr)_3]_4$ (from further hydrogenation of **2a**) with 1–5% of $HRh[P(O\text{-}i\text{-}Pr)_3]_3$. In the benzyl case, the yield of **2b** was 67%, with an additional 7% of **4b** and **5b** in roughly a 1:2 ratio. A small amount of $HRh[P(O\text{-}i\text{-}Pr)_3]_3(PhCH_2NC)$ was also formed, along with $HRh[P(O\text{-}i\text{-}Pr)_3]_3$. Apparently a fragmentation process occurs along with hydrogenation for R = $PhCH_2$.

The results are more complex for the reactions of **1c–e** with hydrogen. The *n*-butyl compound **1c** gives not only a 40% yield (by NMR) of **2c** but also a 30% yield of a 3:2 mixture of **4c** and **5c**. Fragmentation is significant, 20% of the product being $HRh[P(O\text{-}i\text{-}Pr)_3]_3$. No $HRh[P(O\text{-}i\text{-}Pr)_3]_3(n\text{-BuNC})$ is seen, possibly because it was used up in transforming **2c** to **4c** annd **5c**. Nevertheless, the total yield of hydrogenation products was 70%, vs. 74% for R = $PhCH_2$. In the case of R = *t*-Bu and 2,6-$Me_2C_6H_3$, on the other hand, hydrogenation-derived products are formed in less than 30% yield. No **2d** is observed at all, and only 5% of **2e** is formed (at very long reaction times, after exhausting all $HRh[P(O\text{-}i\text{-}Pr)_3]_3(RNC)$). In the case of R = *t*-Bu, **4d** and **5d** are formed in a 1:3 ratio; a 5:1 ratio of **4e** to **5ke** is seen in the 2,6-xylyl case. The major product in both cases is $HRh[P(O\text{-}i\text{-}Pr)_3]_3$ (30–40%), followed by $H(\mu\text{-H})_3Rh_2[P(O\text{-}i\text{-}Pr)_3]_4$.[42] Up to 15% of $HRh[P(O\text{-}i\text{-}Pr)_3]_3(RNC)$ is also formed, but some is undoubtedly lost in generating substitution products. The lack of hydrogenation products suggests that the fragmentation occurs before the first insertion step. A likely candidate is the proposed intermediate $H_4(RNC)Rh_2P_4$ in Schemes III and IV. For the very large *tert*-butyl and 2,6-xylyl isocyanides, insertion into an H–Rh bond might be sterically unfavorable, and fragmentation of the intermediate would eventually occur. Two possible fragments, $[HRhP_2(RNC)]$ and $[H_3RhP_2]$, could be the precursors of the observed products $HRh[P(O\text{-}i\text{-}Pr)_3]_3(RNC)$, $HRh[P(O\text{-}i\text{-}Pr)_3]_3$, and $H(\mu\text{-H})_3Rh_2[P(O\text{-}i\text{-}Pr)_3]_4$.[43] Also, unfavorable steric interaction between the bulky *tert*-butyl or 2,6-xylyl groups and the alkyl groups on the phosphites probably makes the phosphites unusually prone to substitution, either in **2** or in some intermediate step in the hydrogenation. If this is true, then if any **2d,e** is formed at all, substitution reactions may destroy it as fast as it is formed. Thus the steric control seen in other aspects of the chemistry of **1**[24] is seen in its reaction with hydrogen as well.

The compound $(\mu\text{-4-}ClC_6H_4NC)_2Rh_2[P(O\text{-}i\text{-}Pr)_3]_4$ (**6a**)[24] also reacts with hydrogen. One isocyanide appears to be displaced rapidly; NMR monitoring after 1 h showed no trace of **6a** or **1a** but large amounts of **3a** and various products. The eventual products were **2a**, **4a**, and $HRh[P(O\text{-}i\text{-}Pr)_3]_3$ in roughly equal amounts, plus a very small amount of $HRh[P(O\text{-}i\text{-}Pr)_3]_4$. Note that the (hypothetically reversible) reaction

$$H_2(RNC)Rh_2P_4 + RNC = (RNC)_2Rh_2P_4 + H_2$$

(R = 4-ClC_6H_4) is rapid[24] and involves some decomposition to $HRh[P(O\text{-}i\text{-}Pr)_3]_3$. Thus the reaction of **6a** with H_2 presumably involves displacement of RNC by H_2 and further reaction to give **3a**; the displaced isocyanide returns and substitutes for a phosphite at some later step. Since the overall reaction of **6a** is faster than that of **1a** itself and no **1a** or **6a** is seen in the reaction mixture after 1 h, it is reasonable to assume that substitution occurs on **3a** or on the unseen intermediate formed from the second insertion rather than only after **2a** has been formed. It is then possible that the isocyanide-substituted intermediates go on to the eventual products faster than the all-phosphite ones. The removal of the kinetic "bottleneck" after **3a** means that the reaction as a whole will therefore proceed more rapidly.

Conclusion

The reaction of the compounds $(\mu\text{-H})_2(RNC)Rh_2[P(O\text{-}i\text{-}Pr)_3]_4$ with hydrogen has been found to result in the reduction of the isocyanide C≡N triple bond all the way to a single bond, with the formation of $(\mu\text{-H})(\mu\text{-RNMe})Rh_2[P(O\text{-}i\text{-}Pr)_3]_4$. The intermediate formimidoyl complexes $H(\mu\text{-H})_2(RN{=}CH)Rh_2[P(O\text{-}i\text{-}Pr)_3]_4$ can be detected spectroscopically for the cases of R = 4-ClC_6H_4, $PhCH_2$, and *n*-Bu. Further reaction of $(\mu\text{-H})(\mu\text{-RNMe})Rh_2[P(O\text{-}i\text{-}Pr)_3]_4$ with hydrogen slowly liberates the secondary amine RNHMe along with the hydrogen adduct of $(\mu\text{-H})_2Rh_2[P(O\text{-}i\text{-}Pr)_3]_4$. Thus the coordinately unsaturated dimer $(\mu\text{-H})_2Rh_2[P(O\text{-}i\text{-}Pr)_3]_4$ mediates a stoichiometric cycle for the hydrogenation of isocyanides. Steric control is evident at several places in the cycle. Steric factors determine the isocyanide coordination geometry and the dynamic behavior of the compounds $(\mu\text{-H})_2(RNC)Rh_2[P(O\text{-}i\text{-}Pr)_3]_4$. They affect the path of the hydrogenation, bulky isocyanides inhibiting the insertion step and leading to fragmentation reactions. Finally, they affect the viability of the product $(\mu\text{-H})(\mu\text{-RNMe})Rh_2[P(O\text{-}i\text{-}Pr)_3]_4$ under the reaction conditions; the small amounts of hydrogenation products in systems based on bulky isocyanides have a phosphite replaced by isocyanide, the phosphite apparently having been labilized by steric interaction with the isocyanide residue, either after the formation of $(\mu\text{-H})(\mu\text{-RNMe})Rh_2[P(O\text{-}i\text{-}Pr)_3]_4$ or at some intermediate step. This represents only the second case in the $(HRhL_2)_n$ series where a donor ligand has been displaced from the complex with retention of polynuclear character.[44]

The hydrogenation products $(\mu\text{-H})(\mu\text{-RNMe})Rh_2[P(O\text{-}i\text{-}Pr)_3]_4$ were found to undergo H/D exchange with D_2 gas via an intramolecular oxidative addition of certain ligand positions. The selectivity of this process depends on the favorability of formation of a five-membered metallacycle with respect to smaller ring sizes. Rather than being unique to this compound, we expect that this will be found to be a general feature among all the coordinatively unsaturated rhodium complexes in this system.

Experimental Section

Reagents and Methods. All manipulations were performed by using standard Schlenk techniques or in a Vacuum-Atmospheres drybox under argon or nitrogen. Toluene, benzene, pentane, hexane, and tetrahydrofuran were distilled from sodium/benzophenone. Acetonitrile was distilled from P_4O_{10} onto freshly activated 3-Å molecular sieves and then distilled again. 2-Propanol was dried with 3-Å molecular sieves or with sodium isopropoxide and distilled. Deuterated solvents were stored over sodium/potassium/benzophenone and vacuum transferred di-

(42) The $H(\mu\text{-H})_3Rh_2[P(O\text{-}i\text{-}Pr)_3]_4$ was not formed by complete hydrogenation of the isocyanide, as in the hydrogenation of **1a,b**; the same methods used to identify RNHMe in the hydrogenation of the latter compounds detected no *t*-BuNHMe in the reaction of **1d** with hydrogen.

(43) An attempt to prepare $HRh[P(O\text{-}i\text{-}Pr)_3]_2(PhCH_2NC)$ from $ClRh[P(O\text{-}i\text{-}Pr)_3]_2(PhCH_2NC)$ and $KBH(O\text{-}i\text{-}Pr)_3$ gave a similar fragmentation, the major products of which were $HRh[P(O\text{-}i\text{-}Pr)_3]_3$ and $HRh[P(O\text{-}i\text{-}Pr)_3]_3(PhCH_2NC)$.

(44) Price, R. T.; Muetterties, E. L., unpublished results.

rectly into the NMR tube before being sealed. Compounds **1a–e**, $(\mu\text{-H})_2Rh_2[P(O\text{-}i\text{-}Pr)_3]_4$, and $HRh[P(O\text{-}i\text{-}Pr)_3](t\text{-BuNC})$ were prepared according to ref 24. The $4\text{-}ClC_6H_4NC$ was prepared from the corresponding aniline[45] and sublimed immediately before use. Hydrogen and ethylene (Matheson) were used as received.

The ^1H, ^{31}P, and ^{13}C NMR spectra were recorded on 180-, 200-, 250-, or 300–MHz (proton) instruments consisting of Oxford superconducting magnets interfaced to Nicolet computers or on a Bruker AM-500. The ^1H and ^{13}C spectra were referenced to tetramethylsilane. The ^{31}P spectra were referenced to external $P(OMe)_3$ and later corrected to 85% H_3PO_4. The $^2H\{^1H\}$ NMR spectra were recorded on the AM-500 and referenced by using the natural-abundance deuterium resonance of the protio solvent. Positive chemical shifts are downfield in all cases and are expressed in parts per million (δ). IR spectra were taken on a Perkin-Elmer 283 spectrophotometer. Mass spectra were obtained via electron impact (70 eV) by using an AEI MS-12 instrument with an INCOS data system. Elemental analyses were performed by Mr. Vazken H. Tashinian in the U.C. Berkeley Microanalytical Laboratory.

$(\mu\text{-H})(\mu\text{-PhCh}_2\text{NMe})Rh_2[P(O\text{-}i\text{-}Pr)_3]_4$ (2b). A dry reaction tube closed with a Teflon valve was charged with 400 mg (0.345 mmol) of $(\mu\text{-H})_2(PhCH_2NC)Rh_2[P(O\text{-}i\text{-}Pr)_3]_4$ (**1b**). The vessel was evacuated, and 30 mL of toluene was vacuum transferred directly from sodium/benzophenone ketyl. The vessel was filled with 1 atm of hydrogen, and the valve was closed. The solution was stirred at room temperature for 15 days, replenishing the hydrogen atmosphere once. At the end of this time, the solvent was vacuum transferred to another container and saved for analysis for $PhCH_2NHMe$ (vide infra). The greenish solid residue left in the reaction vessel was treated with ca. 10 mL of 2-propanol and filtered to remove the sparingly soluble $(\mu\text{-H})_2Rh_2[P(O\text{-}i\text{-}Pr)_3]_4$, leaving a yellow solution. The solution was cooled to −40 °C to precipitate a few more milligrams of $(\mu\text{-H})_2Rh_2[P(O\text{-}i\text{-}Pr)_3]_4$. The solution was then evaporated to dryness and redissolved in 20 mL of 3:2 acetonitrile/2-propanol. Crystallization at −40 °C gave 220 mg (55%) of yellow crystals in two crops. ^1H NMR (THF-d_8): δ 7.96 (dd, J = 7.0, 1.5 Hz, 2 H, ortho), 6.88 (mult, 3 H, meta + para), 4.86 and 4.72 (mults, 6 H each, methines), 4.58 (br t or quintet, J_{HP} = 9 Hz, 2 H, benzyl), 3.26 (br quintet, J_{HP} = 4 Hz, 3 H, NMe), 1.29, 1.27, 1.23, 1.16 (d, J_{HH} = 6.1 Hz, 18 H each, phosphite methyls), −10.73 (ttt, $J_{HP(trans)}$ = 85.6 Hz, J_{HRh} = 21.1 Hz, $J_{HP(cis)}$ = 10.0 Hz, 1 H, hydride). $^1H\{^{31}P\}$ NMR (THF-d_8): benzyl, δ 4.58, and NMe, δ 3.26, singlets; hydride, δ −10.76 (t, J_{HRh} = 21.0 Hz). ^{13}C NMR (THF-d_8, 10 °C): δ 144.74 (s, ipso), 130.06 (br d, J_{CH} = 155.0 Hz, meta), 126.69 (dd, $^1J_{CH}$ = 156.5 Hz, $^2J_{CH}$ = 7.8 Hz, ortho), 125.54 (dt, $^1J_{CH}$ = 157.9 Hz, $^2J_{CH}$ = 7.6 Hz, para), 67.98 (t, J_{CH} = 133.1 Hz, benzyl), 67.72 and 67.66 (d, J_{CH} = 145 Hz, methines), 52.75 (quartet, J_{CH} = 133.3 Hz, NMe), 25.62, 25.46, 25.28, and 25.07 (quartets, J_{CH} = 125 Hz, phosphite methyls). Anal. Calcd for $C_{44}H_{95}NO_{12}P_4Rh_2$: C, 45.6; H, 8.26; N, 1.21; P, 10.7. Found: C, 45.7; H, 8.23; N, 1.36; P, 10.5.

$(\mu\text{-H})(\mu\text{-4-ClC}_6\text{H}_4\text{NMe})Rh_2[P(O\text{-}i\text{-}Pr)_3]_4$ (2a). Preparation was similar to 2b, except that the reaction was allowed to proceed for only 2 days. The final crystallization was from 20 mL of pure 2-propanol, yielding 360 mg (88%, from 410 mg of starting materials), of yellow crystals. ^1H NMR (toluene-d_8, 20 °C): δ 7.28 (br, $\omega_{1/2} \approx 60$ Hz, 2 H, ortho), 6.99 (br d, J = 7 Hz, 2 H, meta), 4.93 and 4.82 (mults, 6 H each, methines), 3.57 (br, 3 H, NMe), 1.42, 1.37, 1.27, and 1.07 (d, J_{HH} = 6.1 Hz, 18 H each, phosphite methyls), −10.22 (ttt, $J_{HP(trans)}$ = 84.5 Hz, J_{HRh} = 22.2 Hhz, $J_{HP(cis)}$ = 9.9 Hz, 1 H, hydride). $^1H\{^{31}P\}$ NMR (toluene-d_8): NMe, δ 3.57 (s); hydride, δ −10.24 (t, J_{HRh} = 22.2 Hz). ^{13}C NMR (C_6D_6): δ 163.05 (s, ipso or para), 126.12 (br d, J_{CH} = 160.0 Hz, ortho + meta), 123.82 (s, para or ipso), 67.86 and 67.74 (d, J_{CH} = 143 Hz, methines), 46.96 (quartet, J_{CH} = 133.5 Hz, NMe), 25.41, 25.04, and 24.50 (2:1:1, quartet, J_{CH} = 125 Hz, phosphite methyls). Mass spectrum: m/e 1179 and 1181 (M^+, $^{35,37}Cl$). Anal. Calcd for $C_{43}H_{92}ClNO_{12}P_4RH_2$: C, 43.8; H, 7.86; N, 1.19; P, 10.5. Found: C, 43.4; H, 7.88; N, 1.15; P, 10.7.

X-ray Crystallographic Study of 2a. Crystals were grown by cooling a saturated solution in 2-propanol to −40 °C. A platelike crystal was selected, mounted in a glass capillary, and sealed under nitrogen. Precession photographs indicated monoclinic syymmetry and systematic absences consistent with the space group $P2_1/n$ (an alternate setting of $P2_1/c$, no. 14).[46] The final cell parameters were determined from a least-squares fit of 24 well-centered reflections with $2\theta \approx 28°$. Intensity data were collected by using the parameters listed in Table I. Crystal orientation was checked using three reflections measured every 400 data; reorientation was performed twice after check reflections slipped by *ca.* 0.1°. The intensities of three reflections were monitored every 2 h of X-ray exposure to check for decay. A linear, slightly anisotropic decay of 2–4% in intensity was observed but not corrected for. Azimuthal scans of six reflections with high χ showed I_{min}/I_{max} averaging 0.90; an analytical absorption correction based on crystal shape was performed. The positions of the rhodium atoms were deduced from the Patterson map, and all other atoms were located by standard least-squares and Fourier techniques. After refinement of all non-hydrogen atoms with anisotropic thermal parameters, a difference Fourier map showed peaks for many of the hydrogen atoms, but not the hydride. At this point all hydrogen atoms except the hydride were inserted in idealized positions with a C–H bond length of 0.95 Å and given isotropic thermal parameters 10% greater than the equivalent isotropic thermal parameter of the attached carbon. Hydrogen atoms were included in structure factor calculations but not refined. Full-matrix nonlinear least-squares methods were used, the function minimized being $\sum w(|F_o| - |F_c|)^2$, where the weight of a given observation $w = 4F_o^2/[\sigma_o^2(F_o^2) + (pF_o^2)^2]$ with $p = 0.05$. The analytical forms of the scattering factor tables were used, and all non-hydrogen scattering factors were corrected for the real and imaginary components of anomalous dispersion. Examination of F_o vs. F_c for the 19 most intense reflections suggested no effects due to secondary extinction; inspection of the final residuals with respect to ranges of parity, F_o, $(\sin\theta)/\lambda$, hkl, and various projections revealed no unusual trends. Upon convergence, several isopropyl carbons (C111, C112, C113, C73) were undergoing small but apparently random shifts of 0.01–0.02 Å per cycle, possibly indicative of slight disorder; due to their lack of chemical importance, no attempt was made to model this. The largest shift/error for these atoms in the final cycle was 3.2; for all other atoms it was less than 0.7. The final difference Fourier map contained two peaks of ca. 1 e/Å^3 between O10, O11, and O12; all other peaks were less than 0.6 e/Å^3.

Exchange of 2a with D_2. A dry reaction tube closed with a Teflon valve was charged with 100 mg of **2a** and 10 mL of toluene. The solution was degassed on a vacuum line, and the vessel was filled with 2 atm of D_2. The solution was stirred at room temperature for 9 days, with the D_2 atmosphere replaced each day. The solution color changed from yellow to light red. At the end of this period the solvent was vacuum transferred away (the solution turned greenish yellow as the D_2 was removed) and saved for analysis for $4\text{-}ClC_6H_4NHMe$ (vide infra). The solid yellow-green residue was found by ^1H NMR to contain 90% $(\mu\text{-D})(\mu\text{-4-}ClC_6H_4NMe)Rh_2[P(O\text{-}i\text{-}Pr)_3]_4$ and 10% $(\mu\text{-D})_2Rh_2[P(O\text{-}i\text{-}Pr)_3]_4$ by integration of the phosphite methyl and methine regions, but the ratio of methyl to methine was only about 4.5:1. The deuterated **2a** was extracted into acetone for $^2H\{^1H\}$ NMR. In the mass spectrum of the combined residue, the parent ions were not observed, but the region of the free $P(O\text{-}i\text{-}Pr)_3$ fragment showed an envelope of peaks from m/e 208 ($P(OC_3H_7)_3^+$) to 226 ($P(OC_3D_6H)_3^+$).

Detection of RNHMe. The solvent and volatile components from the hydrogenation of **2b** (prepared in situ from **1b**, reaction described above) and the reaction of **2a** with D_2 (described above) were subjected to GC (10% Carbowax 20M/Gaschrom Q, 160 °C for **2b**; capillary column, 120 °C for **2a**) and GC/MS (capillary column, same temperature; 70 eV) analyses. In both cases, the secondary amine RNHMe was detected by both GC and GC/MS; in the case of $PhCH_2NHMe$, the identification was confirmed by comparison with a commercial sample (Fluka). The yields of the amine determined by GC (using a standard for the benzyl compound but using only peak area relative to solvent for the $4\text{-}ClC_6H_4$ compound) were equal to those of $(\mu\text{-H})_2Rh_2[P(O\text{-}i\text{-}Pr)_3]_4$ to within experimental error, but since this assumes that the relatively

(45) Weber, W. P; Gokel, G. W.; Ugi, I. K. *Angew. Chem., Int. Ed. Engl.* **1972**, *11*, 530.

(46) Cromer, D. T.; Waber, J. T. *International Tables for X-ray Crystallography*; Kynoch Press: Birmingham, England, 1974.

Table VI. NMR Data for *cis*-$(\mu$-H)$(\mu$-RNMe)$Rh_2[P(O\text{-}i\text{-}Pr)_3]_3$(R′NC) (4)

parameter[a]	4a	4e	4f
δ_H	−8.78	−9.73	−9.35
J_{HA}	12.6	10.9	12.0
J_{HB}	82.0	89.8	82.0
J_{HC}	90.2	89.8	86.4
$J_{HX,Y}$	22.3	22.5	22.2
δ_A	155.6	156.2	156.4
δ_B	137.0	138.7	137.4
δ_C	128.3	131.2	129.5
J_{AB}	69.6	70	70.0
J_{AC}	6.4	8	5.8
J_{BC}	89.7	87	88.5
J_{AX}	245.4	256	246.3
J_{BX}	291.3	292	289.0
J_{CY}	290.2	298	296.6
J_{AY}	1.7		
J_{BY}	8.6	8	7.6
J_{CX}	8.0	8	6.3

[a] For labeling scheme, see Scheme VI. J values in hertz.

involatile amines were quantitatively removed from the reaction mixture, the yield of $(\mu\text{-H})_2Rh_2[P(O\text{-}i\text{-}Pr)_3]_4$ is the more precise and is the one quoted in the text.

Reaction of 2a with 4-ClC_6H_4NC. To a solution of 50 mg (0.042 mmol) of **2a** in 10 mL of THF was added a solution of 5.8 mg (1.0 equiv) of 4-ClC_6H_4NC in 5 mL of THF over about 1 min. The solution rapidly turned red and then reddish brown after about 10 min. The solution was evaporated to dryness and redissolved in toluene-d_8 for NMR. In addition to $HRh[P(O\text{-}i\text{-}Pr)_3]_3$(4-$ClC_6H_4NC$), $HRh[P(O\text{-}i\text{-}Pr)_3]_4$, **2a**, and $(\mu$-4-$ClC_6H_4NC)_2Rh_2[P(O\text{-}i\text{-}Pr)_3]_4$, 45% (mole fraction) of **4a** was observed. Data for **4a**: ^1H NMR δ 7.34, 7.02, 7.01, and 6.82 (d, J = 8.5 Hz, 2 H each, aryls), 5.3–4.8 (overlapping mults, 9 H, methines), 3.31 (br, 3 H, NMe), 1.38, 1.37, 1.31, 1.22, 1.07, and 1.04 (d, J = 6.1 Hz, 9 H each, phosphite methyls). Hydride and $^{31}P\{^1H\}$ NMR data are given in Table VI. Selectively alkyl proton decoupled (hydride-coupled) ^{31}P NMR: P_A broadens, P_B and P_C split further into doublets (J_{HB} = 81 Hz, J_{HC} = 90 Hz).

Reaction of 2a with $HRh[P(O\text{-}i\text{-}Pr)_3]_3(t\text{-}BuNC)$. A 5-mm NMR tube was charged with 20 mg (0.017 mmol) of **2a** and 14 mg (0.017 mmol) of $HRh[P(O\text{-}i\text{-}Pr)_3]_3$ (t-BuNC); toluene-d_8 was vacuum distilled in, and the tube was sealed. The mixture was allowed to react at room temperature and monitored by NMR. The starting material resonances were observed to shrink and those due to **4f**, **5f**, and $HRh[P(O\text{-}i\text{-}Pr)_3]_4$ grew in, along with a small amount of $HRh[P(O\text{-}i\text{-}Pr)_3]_3$ (6% after 45 days) due to thermal decomposition. Data for **4f**: ^1H NMR δ 7.36 and 7.00 (d, J = 8.9 Hz, 2 H each, aryls), 5.24 and 4.90 (1:2, mults, 9 H total, methines), 3.34 (br, 3 H, NMe), 1.39, 1.34, 1.32, 1.25, and 1.08 (2:1:1:1:1, d, J = 6.1 Hz, 54 H total, phosphite methyls), 1.23 (s, 9 H, t-Bu). Hydride and $^{31}P\{^1H\}$ NMR data are given in Table VI. Data for **5f**: ^1H NMR: δ −11.47 (dtdd, $J_{HP(trans)}$ = 85 Hz, J_{HRh} = 22 Hz, $J_{HP(cis)}$ = 14, 8 Hz).

Spectroscopic Monitoring of the Reactions of 1 with H_2. Typical experiments used 20 mg of **1a–e** in toluene-d_8 (or protiotoluene for ^2H NMR) sealed under 700 torr (4–6 equiv) of H_2 or D_2. The mixture was kept frozen until monitoring was to begin. Species observed for which data is not listed elsewhere include the following. **2c**: ^1H NMR δ 5.0 (overlapping mults, methines), 3.47 (overlapping mults, 5 H, NMe + n-Bu α), 1.46, 1.37, and 1.36 (1:1:2, d, J = 6.1 Hz, total 72 H, phosphite methyls), 1.01 (t, J = 7.4 Hz, 3 H, n-Bu δ), −10.24 (ttt, $J_{HP(trans)}$ = 85.4 Hz, J_{HRh} = 21.1 Hz, $J_{HP(cis)}$ = 9.6 Hz). $^{31}P\{^1H\}$ NMR (see text for labeling scheme): P_B, δ 151.0, P_A, δ 135.6 ($|J_{AX} + J_{AX'}|$ = 321 Hz, $|J_{BX} + J_{BX'}|$ = 227 Hz, $|J_{AB} + J_{AB'}|$ = 87 Hz). **2e**: $^{31}P\{^1H\}$ NMR: P_B, δ 152.98, P_A, δ 137.4 ($|J_{BX} + J_{BX'}|$ = 239.5 Hz, $|J_{AB} + J_{AB'}|$ = 73.2 Hz). **3a**: ^1H NMR δ 10.10 (dd, J_{HP} = 36.2, 27.9 Hz, 1 H, RNCH), 7.48 and 7.18 (d, J = 8.8 Hz, 2 H each, aryls), 5.1–5.0 (overlapping mults, 12 H, methines), 1.35, 1.33, 1.29, and 1.13 (d, J = 6.1 Hz, 18 H each, phosphite methyls), −8.66 (mult, 2 H, bridging hydrides), −18.53 (mult, 1 H, terminal hydride). $^1H\{^{31}P\}$ NMR: formimidoyl, δ 10.10 (br s, $\omega_{1/2}$ = 8 Hz); hydrides, δ −8.67 (td, J_{HRh} = 18 Hz), −18.54 (d of quartets, $^1J_{HRh}$ = 18.1 Hz, $^3J_{HRh} = J_{HH}$ = 3.3 Hhz). $^{31}P\{^1H\}$ NMR (see Figure 4 for labeling scheme): P_A, δ 145.1 (d, J_{AX} = 338 Hz, of mults), P_B, δ 158.9 (ddd, J_{BX} = 164 Hz, J_{AB} = 64 Hz, J_{BY} = 16 Hz, of mults, J_{BC} < 6 Hz), P_C, δ 157.5 (dd, J_{CY} = 185 Hz, J_{AC} = 34 Hz). **3b**: $^1H\{^{31}P\}$ NMR δ 8.6 (1 H), −8.89 (t, J_{HRh} = 16.2 Hz, 2 H), −17.85 (d, J_{HRh} = 16.1 Hz, of mults, 1 H). **3c**: ^1H NMR δ 9.10 (dd, J_{HP} = 36, 31 Hz, 1 H), −8.9 (br mult, 2 H), −17.8 (mult, 1 H). **4b**: $^1H\{^{31}P\}$ NMR δ −9.54 (t, J_{HRh} = 21.6 Hz). **4c**: ^1H NMR δ −8.63 (mult). **4d**: ^1H NMR δ −9.73 (ttd, $J_{HP(trans)}$ = 89.8 Hz, J_{HRh} = 20.4 Hz, $J_{HP(cis)}$ = 10.9 Hz). **4e**: ^1H and $^{31}P\{^1H\}$ NMR data given in Table VI. **5b**: $^1H\{^{31}P\}$ NMR δ −11.50 (dd, J_{HRh} = 23.7, 20.1 Hz). **5c**: ^1H NMR δ −11.22 (mult). **5d**: ^1H NMR δ −11.69 (ddddd, $J_{HP(trans)}$ = 89.7 Hz, J_{HRh} = 23.0, 19.2 Hz, $J_{HP(cis)}$ = 14.1, 5.2 Hz).

Acknowledgment. This work was sponsored by the National Science Foundation in the form of a research grant (CHE 830-7159) and a predoctoral fellowship for S.T.M. We thank Dr. Frederick J. Hollander of the U.C. Berkeley X-ray crystallographic facility (CHEXRAY) for assistance with the crystal structure. Johnson-Matthey Inc. provided a generous loan of $RhCl_3 \cdot 3H_2O$.

Registry No. **1a**, 104215-46-5; **1b**, 104215-47-6; **1c**, 104215-48-7; **1d**, 104215-49-8; **1e**, 104215-50-1; **2a**, 104215-51-2; **2b**, 104215-52-3; **2c**, 104215-37-4; **2d**, 104266-50-4; **2e**, 104215-38-5; **3a**, 104215-39-6; **3b**, 104215-40-9; **3c**, 104215-41-0; **4a**, 104215-55-6; **4b**, 104215-42-1; **4c**, 104215-43-2; **4d**, 104215-44-3; **4e**, 104215-45-4; **4f**, 104320-67-4; **5b**, 104319-31-5; **5c**, 104319-32-6; **5d**, 104319-33-7; **5f**, 104215-57-8; $(\mu\text{-H})_2Rh_2[P(O\text{-}i\text{-}Pr)_3]_4$, 70727-44-5; $HRH[P(O\text{-}i\text{-}Pr)_3]_3$(4-$ClC_6H_4NC$), 104215-53-4; $HRh[P(O\text{-}i\text{-}Pr)_3]_4$, 92226-80-7; $(\mu$-4-$ClC_6H_4NC)_2Rh_2[P(O\text{-}i\text{-}Pr)_3]_4$, 104215-54-5; $HRh[P(O\text{-}i\text{-}Pr)_3]_3$(Bu-$t$-NC), 104215-56-7; $H(\mu\text{-H})_3Rh_2[P(O\text{-}i\text{-}Pr)_3]_4$, 70727-45-6; 4-$ClC_6H_4NC$, 1885-81-0; (4-$ClC_6H_4$)NHMe, 932-96-7; $PhCH_2NHMe$, 103-67-3.

Supplementary Material Available: Tables of anisotropic thermal parameters for non-hydrogen atoms and hydrogen atom positions and isotropic thermal parameters for $(\mu$-H)$(\mu$-4-$ClC_6H_4NMe)Rh_2[P(O\text{-}i\text{-}Pr)_3]_4$ (6 pages); a listing of observed and calculated structure factors for $(\mu$-H)$(\mu$-4-$ClC_6H_4NMe)Rh_2[P(O\text{-}i\text{-}Pr)_3]_4$ (42 pages). Ordering information is given on any current masthead page.